

# Morphology of Star Formation Regions in Irregular Galaxies

Noah Brosch<sup>1</sup>

Space Telescope Science Institute  
3700 San Martin Drive  
Baltimore MD 21218, U.S.A.

and

Ana Heller and Elchanan Almoznino  
The Wise Observatory and the School of Physics and Astronomy  
Tel Aviv University, Tel Aviv 69978, Israel

Received \_\_\_\_\_; accepted \_\_\_\_\_

---

<sup>1</sup>On sabbatical leave from the Wise Observatory and the School of Physics and Astronomy, Raymond and Beverly Sackler Faculty of Exact Sciences, Tel Aviv University, Tel Aviv 69978, Israel

## ABSTRACT

The location of HII regions, which indicates the locus of present star formation in galaxies, is analyzed for a large collection of 110 irregular galaxies (Irr) imaged in H $\alpha$  and nearby continuum. The analysis is primarily by visual inspection, although a two-dimensional quantitative measure is also employed. The two different analyses yield essentially identical results. HII regions appear preferentially at the edges of the light distribution, predominantly on one side of the galaxy, contrary to what is expected from stochastic self-propagating star formation scenarios. This peculiar distribution of star forming regions cannot be explained by a scenario of star formation triggered by an interaction with extragalactic gas, or by a strong one-armed spiral pattern.

*Subject headings:* galaxies: irregular - galaxies: stellar content - HII regions - stars: formation

## 1. Introduction

The star formation (SF) is a fundamental process in the evolution of galaxies and is far from being well understood. The SF is usually characterized by the initial mass function (IMF) and the total SF rate (SFR), which depends on many factors such as the density of the interstellar gas, its morphology, its metallicity, *etc.* Generally, four major factors drive star formation in galaxies: large scale gravitational instabilities, cloud compression by density waves, compression in a rotating galactic disk due to shear forces, and random gas cloud collisions. In galaxies with previous stellar generations additional SF triggers exist, such as shock waves from stellar winds and supernova explosions. In dense environments, such as clusters of galaxies and compact groups, tidal interactions, collisions with other galaxies, ISM stripping, and cooling flow accretion probably play some role in triggering the SF process. The triggering mechanisms were reviewed recently by Elmegreen (1998).

While “global” phenomena play a large part in grand design spirals, random collisions of interstellar clouds have been proposed as one explanation for dwarf galaxies with bursts of SF. Due to their small size, lack of strong spiral pattern, and sometimes solid-body rotation (*e.g.*, Martimbeau *et al.* 1994, Blok & McGaugh 1997), the star formation in dwarf galaxies cannot be triggered by compression from gravitational density waves or by disk shear. Therefore, understanding SF in dwarf galaxies should be simpler than in other types of galaxies, because the number of possible trigger mechanisms is reduced.

The H $\alpha$  emission from a galaxy measures its ongoing SFR (Kennicutt 1983, Kennicutt *et al.* 1994). The blue luminosity of a galaxy measures its SF integrated over the last  $\sim 10^9$  yrs (Gallagher *et al.* 1984). The red continuum radiation originates both from relatively young stars which already evolved into red giants and super-giants, and from a large population of aged low-mass stars, if previous SF episodes took place.

Hunter *et al.* (1998) tested a set of SF predictors on two small samples of dwarf galaxies, one observed by them and another derived from de Blok (1997). They found that the ratio of HI surface density to the critical density for the appearance of ring instabilities did not correlate with the star formation, but that the stellar surface brightness did. From this, they concluded that possibly some stellar energy input provides the feedback mechanism for star formation. Brosch *et al.* (1998) confirmed that the strongest correlation among a number of parameters tested on a sample of Virgo cluster dwarf irregular galaxies was between the average H $\alpha$  surface brightness and the mean blue surface brightness. This is similar to the findings of Phillipps & Disney (1985) for spiral galaxies, where in a sample of 77 spiral galaxies from Kennicutt & Kent (1983) a correlation was found between the total H $\alpha$  emission (expressed as specific SFR or as H $\alpha$  equivalent width) and the average blue surface brightness.

On the level of individual HII regions in dwarf irregular galaxies, Heller *et al.* (1998: HAB98) showed that a correlation exists also between the H $\alpha$  line flux and the red continuum flux underneath the region, measured with the same aperture as the line flux. We emphasize that in this case the correlation is between local quantities, not for overall galactic properties. These correlations indicate that the regulation of SF in Irr's is local and by the existing stellar population. The self-regulated evolution of dwarf galaxies has recently been modeled by Andersen & Burkert (1997).

We concentrate here on samples of late-type dwarf irregular galaxies (DIGs) in the Virgo cluster (VC) and elsewhere in the nearby (within 100 Mpc) Universe. The reason for selecting DIGs is to limit the number of possible SF trigger mechanisms; DIGs are devoid of large-scale SF triggers, as explained above. We take advantage of the availability of net H $\alpha$  line images to determine the general pattern of the distribution of HII regions over the irregular galaxies. As far as we could ascertain, such a study of a large sample of irregular galaxies was never published. Previous attempts to classify

DIGs were *e.g.*, by Sandage & Binggeli (1984) for low surface brightness (LSB) objects, by Loose & Thuan (1985) for BCDs, and by Patterson & Thuan (1996) for DIGs. All used broad-band images to perform the classification.

We do not study here the morphology of the galaxies, as reflected by their light distribution on broad-band images, but rather the morphology of their ensemble of HII regions. Our goal is to gain some insight on the star-forming properties of this class of galaxies. The question of the spatial distribution of HII regions in irregular galaxies has been studied previously by Hodge (1969) for seven nearby objects, and by Hunter & Gallagher (1986) for a larger sample of galaxies.

## 2. The samples

The primary sample consists of 52 DIGs in the VC with HI measurements from Hoffman *et al.* (1987, 1989). The sample was constructed in order to enable the detection of weak dependencies of the star formation properties on the hydrogen content and on the surface brightness. We selected two sub-samples by surface brightness; one represents a high surface brightness (HSB) group and is classified as either BCD or anything+BCD, and another represents a low surface brightness (LSB) sample and includes only ImIV or ImV galaxies. The uniform morphological classification, which bins the DIGs in the HSB or LSB groups, is exclusively from Binggeli *et al.* (1985, VCC). The galaxies were observed at the Wise Observatory (WO) from 1990 to 1997, with CCD imaging through broad bands and narrow  $\text{H}\alpha$  bandpasses in the rest frame of each galaxy. The discussion of all observations and their interpretation is the subject of other papers (AB98, HAB98). We restrict the discussion here to the localization of the star-forming regions on the broad-band, or continuum light images of the DIGs. In some Virgo galaxies we did not detect  $\text{H}\alpha$  emission; these objects have been omitted in Table 1 leaving 30 DIGs from our combined Virgo sample.

The two Virgo cluster samples are augmented here by 83 irregular galaxies for which data were collected from the literature. Not all these objects are dwarfs but all appear to be, or are classified as, irregular galaxies; we call them here DIGs and are not strict in qualifying an object as “dwarf”. Three objects of the extended sample appear in two references; these objects have been classified independently and have two entries in Table 1. The total number of classifications is thus 124, but only 110 different objects have been considered.

We inspected H $\alpha$  and broad-band or red continuum images from Strobel *et al.* (1991), Miller & Hodge (1994), McGaugh *et al.* (1995), van Zee (1996), Marlowe *et al.* (1997), Martin (1997), Hilker *et al.* (1998), and Gavazzi *et al.* (1998). The images from van Zee include objects analyzed in her PhD thesis (van Zee 1996) and some galaxies from an unpublished comparison sample. The objects were selected to be LSB DIGs and were checked not to show obvious signs of interaction on the Palomar Sky Survey plates. The objects from van Zee contribute 27 galaxies to the extended sample. The objects studied by Gavazzi *et al.* (1998) and included here consist of eight galaxies classified as Irr, most in the A1367 cluster. The Hilker *et al.* (1997) object is an LMC-like galaxy in the Fornax cluster. Ho II was studied in detail by Puche *et al.* (1992); we used the published images for the present classification. The 12 galaxies studied by Marlowe *et al.* (1997) are classified as either amorphous or blue compact, are intrinsically faint (*i.e.*, dwarf), and are nearby. The sample of Martin (1997) contains a heterogeneous assemblage of star-forming dwarf galaxies. Three objects with spiral morphology (N2537, VII Zw403, and N4861) from her list were excluded from the present analysis, leaving 12 galaxies to be considered here. Additionally, four objects were added from the study of dwarf galaxies in the M81 system (Miller & Hodge 1994) and four other from the study of DIGs by Strobel *et al.* (1991). Finally, we included 13 objects from the morphological study of LSB disk galaxies of McGaugh *et al.* (1995) which did not show strong spiral patterns on the published images.

The only restrictions to the inclusion of a galaxy in the extended sample were that the object should be classified as an irregular galaxy in the original publication and that it would have a net H $\alpha$  and an off-line image. This resulted in a very heterogeneous collection of irregular galaxies; those from Martin (1997) and Marlowe *et al.* (1997) are mainly low-luminosity, nearby objects, while those from Gavazzi *et al.* (1998), being at  $\sim$ 70 Mpc, are of high luminosity and would not be strictly classifiable as “dwarfs”. Most of the galaxies in Gavazzi *et al.* were rejected because they were not Irr galaxies and so were all the objects analyzed by Hunter *et al.* (1998), which do not have published images but only azimuthal averages of line and continuum emission. We could not use the large H $\alpha$  and continuum image set in Koopman (1997) because it contains only spiral and lenticular galaxies. The entire selection of 110 galaxies classified here is listed in Table 1, where the objects from our Virgo sample are identified by their number in the Virgo cluster catalog (Binggeli *et al.* 1985).

### 3. Analysis and results

The analysis reported here is based primarily on the visual inspection of the net H $\alpha$ -line and off-line images of each galaxy. These are usually presented side-by-side in the original publications, at the same scale and with enough “gray-scale stretch” to allow easy perception of the HII regions on the net-line image, and of the general outline of the galaxy in the off-line image. This facilitates the comparison and the determination of whether the HII regions are distributed mostly at the edges or near the center of an object. These two cases have been noted in Table 1 as E for edge and C for center, and are the primary morphological index used for this classification.

There are a few cases of mixed morphology, which have been so noted in Table 1. One such example is UGC 7178, from the primary sample of van Zee (1996), which has four HII regions, two near the center and two at the edge and is classified here as

C+E. Other galaxies do not show preferential SF at either the center or the edge, but display a  $\sim$ linear distribution of HII regions showing up as a “spine” on the galaxy image. These objects are noted as L=linear, and/or Sp=spine types and are probably related to the “cometary” galaxies noted by Loose & Thuan (1985). A few objects have a number of HII regions arranged on the (partial) circumference of an ellipse; these are marked El=ellipse in Table 1. Finally, some Irr’s show a scattering of HII regions and are accordingly marked D=diffuse. UGC11820 in van Zee’s primary sample (van Zee 1996) has its HII regions arranged on  $\sim$ a spiral arm. It is possible that this is a case of mistaken classification and the object is probably a spiral, as listed in UGC and in NED. A similar case may be object 127037 in Gavazzi *et al.* (1998).

Our classification, by the distribution of the visible HII regions, should be compared with that of Patterson & Thuan (1996), where six classes of DIGs were distinguished on the basis of broad-band B and I images. The classifications are an extension of the Loose & Thuan (1986) scheme and bin the DIGs into dwarf spirals (dS), nucleated dwarf irregulars (dInE), dwarf ellipticals with a central ridge (dIrE), dwarfs with “asymmetric star formation” (dIa), objects with randomly scattered star formation similar to the GR8 galaxy (GR8), and dwarfs which show a bar with wispy extensions (dIB). The two UGC objects in common, U300 and U2162, have both been classified by Patterson & Thuan as dIa, while we classify them as E and A, confirming the asymmetry mention and adding the qualifier that the HII regions tend to be at the edges of the galaxies.

We used a second morphological index to flag a symmetric or asymmetric distribution (S/A) of HII regions. A galaxy is labelled asymmetric (A) in the distribution of its HII regions if these are located predominantly on one side of the galaxy. In other words, the label A is assigned if it is possible to draw on the continuum or broad-band image of a galaxy a diameter which bisects it so that most of the HII regions are on one side of this diameter. If no such diameter seems to exist, the galaxy is classified as symmetrical

(S) in the distribution of its HII regions. This asymmetry criterion is similar to that used by Hodge (1969), with the exception that Hodge used the “reference frame” of the HII region distribution while we used that of the red continuum light. Note that the secondary classification of the asymmetry is independent of the primary classification of edge/center/spine described above. This secondary classifying index is also listed in Table 1. In some cases the images were too poor to allow a classification. These objects have a question mark in the table. The references for the images are listed in Table 2.

We show in Figure 1 examples of the primary and secondary classifications using objects from AB98 and HAB98. The top row shows an object with edge distribution of HII regions, which is asymmetric. The middle row shows a galaxy where the HII regions are arranged in a linear, spine-like configuration. The bottom row shows an object with a centrally located, symmetric distribution of HII regions.

Obviously, a consistent classification requires similar types of display, contrast of images, *etc.* This is not always the case, as some sources did not provide two images (line and continuum) for a galaxy, but only one with overlaid contours for the missing information (*e.g.*, Martin 1997 or Marlowe *et al.* 1997) and we also did not have control over the display mode. Nevertheless, the few galaxies appearing in two references allow some measure of confidence in the classification: N1800, N5253, and II Zw40 are common to the samples from Marlowe *et al.* (1997) and Martin (1997); their classification, performed completely independently on different images, is virtually identical for all three cases.

To put the classification on a more “objective” and numerical basis, and to avoid possible biases caused by the tendency to detect structures when visually inspecting random distributions of dots, we formed two indices which quantify the degree of concentration of HII regions (“concentration index”=CI) and the amount of asymmetry in the HII region distribution (“asymmetry index”=AI). These indices are calculated

from counts of HII identified in various regions of the galaxies’ net-line images we inspected and are listed in Table 1. The definition of these two parameters is fairly intuitive and is explained below.

CI is defined as the ratio of the number of HII regions in the inner part of the galaxy to that in the outer part. We count the HII regions within half the semi-major axis from the center, and divide this by one-quarter of the number of HII regions external to this region. The one-quarter factor brings the comparison to a number per equal-area basis and is, in fact, a ratio of the number surface density of HII regions. CI can have values between zero and infinity, as the outer part of the galaxy may be devoid of HII regions. A value of unity represents a uniform distribution of HII regions, while galaxies with no emission near the center have  $CI=0$ . Galaxies with emission localized in their centers and no emission detected in their outer parts have  $CI=\infty$ ; this is represented in the Table as  $CI=100$ .

The asymmetry index AI is defined as the ratio of the number of HII regions counted in the “HII poor” half of the galaxy to that in the “HII rich” area, where the divider is the bisecting diameter selected visually to show the largest contrast between the two galaxy halves. AI ranges from 0 to 1, with unity representing a symmetric distribution of HII regions. The smaller the value of AI, the more asymmetric is the distribution of HII regions.

We explain the two-dimensional morphological classification with the example of VCC 17, shown in the top row of images in Fig. 1. VCC 17 has two central HII regions and four regions in its outer part. Its CI is therefore  $\frac{2}{4/4} = 2$ . A diameter may be drawn on the figure which puts two HII regions on one side of it and four on the other side. This appears to be the most extreme asymmetry, making  $AI=\frac{2}{4}=0.5$ .

#### 4. Discussion

Our choice of irregular galaxies in which to study the patterns of star formation was quite deliberate. As mentioned in the introduction, these objects should be devoid of large-scale SF triggering mechanisms such as density waves or various disk instabilities. Therefore the triggering mechanisms should be simpler to disentangle in this kind of objects. The star formation indicator used here was the  $\text{H}\alpha$  line emission and the distribution of the HII regions was checked against the light distribution of either the red continuum, or any broad-band images supplied by the authors of a specific paper.

The summary statistic for the distribution among types and the symmetric or asymmetric morphologies is presented in Table 3. The galaxies with mixed morphologies have been counted once in each bin, thus the total number of cases listed in the table is larger than the number of actual galaxies inspected. Galaxies with incomplete or dubious classification, which have only a question mark in the S/A column of Table 1, have been excluded from the statistic. Table 3 shows that most galaxies have an E-type distribution of HII regions. Specifically, we find that about half of all classifications are E and A. The only other bin populated by a significant amount of irregular galaxies is C and S ( $\sim$ one quarter of all classifications) and the other bins are essentially empty. Most galaxies, which were selected only to be irregulars based on their appearance on broad-band images, form preferentially their HII regions in their outer regions (type A has  $\sim$ 2/3 of the cases). The objects in which the distribution of HII regions appears symmetrical are mostly those where it is also central. This is very similar to what Loose & Thuan (1985) found for BCDs.

We show the distribution of the two morphological indices in Figures 2 and 3 (the latter shown to emphasize the behavior of the morphological indices for  $\text{CI} \simeq 0$ ). It is clear that there is a strong dychotomy, because of the objects with essentially central  $\text{H}\alpha$  emission which make up the rightmost part of the plot ( $\text{AI} \simeq \infty$ ). The distribution

of the objects with inner **and** outer HII regions is shown in Figure 4. The figure shows the dominance of the highly asymmetric coverage of DIGs by HII regions, with most cases concentrating at  $AI \leq 0.5$ . This implies that in most DIGs one half of the galaxy has twice or more the number of HII regions than the other half.

Gerola & Seiden (1978) proposed that the mechanism regulating the SF in Irr's is the stochastic self-propagating SF (SSPSF). Their simulations, as well as the more recent ones by Jungwiert & Palous (1994), produce preferentially flocculent or grand-design spirals. If such a mechanism operates in DIGs it should produce an expanding SF wave which would engulf the entire galaxy, or at least those regions with suitable ISM density. Unfortunately, the 3D simulations of SSPSF relevant to DIGs (Comins 1983, 1984) do not show “snapshots” of the SF proceeding with time through the galaxy. Such plots could have been analyzed in a similar manner to the galaxy images and possibly some constraint could have been derived. The few papers which do show such plots (*e.g.*, Gerola *et al.* 1980) have too few figures to make their analysis statistically significant. Note also that in large, slowly-rotating disks, like the LMC, the SSPSF tends to produce mostly long filaments of young stars which show no special preference of galactic location (Feitzinger *et al.* 1987).

If the galaxy is small, and a number of SNs explode off its center, it is possible in principle to have a compression wave travel through the gas and form stars in suitable location while escaping from the galaxy in places where the ISM is thin or altogether absent. It is difficult to estimate the likelihood of such a mechanism but it is possible to examine it in a well-resolved object. The nearby DIG Ho II was studied intensively by Puche *et al.* (1992). A comparison of their H $\alpha$  and off-line images shows that Ho II forms stars near its center. The HI synthesis map indicates that the H $\alpha$  emission originates either at the interfaces between large holes in the HI distribution or in the small HI holes. Thus this case also does not argue in favour of the SSPSF forming stars

asymmetrically, or at the edges of a galaxy.

If the ISM in an irregular galaxy is preferentially aligned with its long dimension, a spine of HII regions could form by the SSPSF mechanism. Similarly, if the galaxy is in a symmetrical gravitational potential well, its ISM could concentrate at the bottom of the potential and begin forming stars there in a C configuration.

Is there a mechanism of SF which would produce predominantly lop-sided regions of SF at the edge of a galaxy ? The question was posed recently for the LMC by de Boer *et al.* (1998), who proposed a mechanism to explain the observed distribution of giant SF structures lining the edge of the LMC. They postulate that the interaction between the LMC gas and gas in the halo of the Milky Way causes gas compression followed by star formation. The SF takes place at the interface between the two gas distributions, where the interaction beween the LMC gas and the MW gas occurs. The rotation of the LMC moves the regions with newly formed stars away from the place of formation, the star formation ceases, and the newly formed stars simply age.

We tested this possibility with the objects in our Virgo samples which have measurements of H $\alpha$  and underlying red continuum emission for individual HII regions. The test is reported in detail in HAB98. If the mechanism of de Boer *et al.* (1998) is at work, we expect a decrease of the H $\alpha$  line intensity simultaneously with an enhancement of the red stellar continuum under the HII region as it ages. The test we performed involved a comparison of the ratios of H $\alpha$  intensities and of the red continua for the brightest and the faintest HII regions identified in the same galaxy. These ratios were compared for 13 objects with multiple HII regions and a trend in the opposite direction from that expected was found; the more intense the underlying red continuum, the stronger the line emission is. This argues against the de Boer *et al.* (1998) proposition and in favour of a mechanism regulating the star formation through the existing local stellar population.

McGaugh *et al.* (1995) mention that the  $m=1$  density wave mode may be possible in LSB galaxies, giving rise to one-armed spirals. In principle, it is possible that the excess of irregulars with asymmetric, edge-concentrated star formation is due to this phenomenon, but we deem it unlikely. The reason is that if the SF process would be driven by a density wave, the one-armed spiral pattern should be visible not only in the distribution of HII regions but also in the red continuum image.

A possibly related phenomenon, of displaced light centers with respect to the outermost isophotes in a sample of extremely late-type spirals was recently reported by Matthews & Gallagher (1997). The phenomenon was explained as a consequence of the disk, which is the luminous galaxy, orbiting in an off-center position within an extended dark halo (Levine & Sparke 1998). The question of dark matter (DM) halos in the context of irregular galaxies has also been discussed by Hunter *et al.* (1998), where the conclusion was that the DM may affect the star formation by enhancing the gravitational potential. It is possible that such a model could explain also the asymmetric patterns of star formation which we reported above, but its exploration, with special emphasis on local density enhancements by the DM, is beyond the scope of this paper.

## 5. Conclusions

We analysed the distribution of regions where star formation takes place at present in a sample of 110 irregular galaxies. Our results can be summarized as follows:

1. Star formation takes place predominantly at the edges of dwarf irregular galaxies, mostly to one side of a galaxy.
2. Existing models of star formation in such objects do not predict such a distribution of star forming regions over a galaxy.

3. The proposals of de Boer *et al.* (1998), of an interaction between the galaxy and some surrounding medium which compresses the ISM and thus enhances the star formation, and of McGaugh *et al.* (1995), of strong single-arm spiral patterns in dwarf galaxies which could give rise to asymmetric distribution of star-forming regions, can probably be rejected.
4. No good explanation was identified for the peculiar location of the HII regions in irregular galaxies.

### Acknowledgements

NB is grateful for continued support of the Austrian Friends of Tel Aviv University and for the hospitality of the Space Telescope Science Institute, where most of this paper was written. EA is supported by a special grant from the Ministry of Science to develop TAUVEX, a UV imaging experiment. AH acknowledges support from the US-Israel Binational Science Foundation and travel grants from the Sackler Institute for Astronomy. Astronomical research at Tel Aviv University is partly supported by a grant from the Israel Science Foundation. Discussions on this subject with Mario Livio appreciated. We are grateful for constructive remarks on this subject from Lyle Hoffman, Crystal Martin, and an anonymous referee. Liese Van Zee and Giuseppe Gavazzi kindly supplied electronic copies of images from their samples of galaxies, used for some of the comparisons presented here.

## References

Almoznino, E. & Brosch, N. 1998, MNRAS, in press (AB98).

Andersen, R.-P. & Burkert, A. 1997, ApJ, preprint.

Brosch, N., Heller, A. & Almoznino, E. 1998, ApJ, 504 (september 10), in press.

Binggeli, B., Sandage, A. & Tamman, G.A. 1985, AJ, 90, 1681.

Comins, N.F. 1983, ApJ, 266, 543.

Comins, N.F. 1984, ApJ, 284, 90.

de Blok, E. & McGaugh, S.S. 1997, MNRAS 290, 533.

de Boer, K.S., Braun, J.M., Vallenari, A. & Mebold, U. 1998, A&A, 329, L49.

Gerola, H. & Seiden, P.E. 1978, ApJ, 223, 129.

Gerola, H., Seiden, P.E. & Schulman, L.S. 1980, ApJ, 242, 517.

Gallagher, J.S., Hunter, D.A. & Tutukov, A.V. 1984, ApJ, 284, 544.

Gavazzi, G., Catinella, B., Carraso, L. Boselli, A. & Contursi, A. 1998, AJ, 115, 1745.

Elmegreen, B.G. 1998, in *Origins of Galaxies, Stars, Planets and Life* (C.E. Woodward, H.A. Thronson, & M. Shull, eds.), ASP series, in press.

Feitzinger, J.V., Haynes, R.F., Klein, U., Wielebinski, R. & Perschke, M. 1987, *Vistas in Astr.*, 30, 243.

Heller, A., Almoznino, E. & Brosch, N. 1998, MNRAS, submitted (HAB98).

Hilker, M., Bomans, D.J., Infante, L. & Kissler-Patig, M. 1997, A&A, 327, 562.

Hodge, P. 1969, ApJ, 156, 847.

Hoffman, G.L., Helou, G., Salpeter, E.E., Glosson, J. & Sandage, A. 1987, ApJS, 63, 247.

Hoffman, G.L., Lewis, B.M., Helou, G., Salpeter, E.E. & Williams, H.L. 1989, ApJS, 69, 65.

Hunter, D.A. & Gallagher, J.S. 1986, PASP, 98, 5.

Hunter, D.A., Elmegreen, B.G. & Baker, A.L. 1998, ApJ, 493, 595.

Jungwiert, B. & Palous, J. 1994, A&A, 287, 55.

Kennicutt, R.C. 1998, ApJ, 498, 541.

Kennicutt, R.C. 1983, ApJ, 272, 54.

Kennicutt, R.C., Tamblyn, P. & Congdon, C.W. 1994, ApJ, 435, 22.

Levine, S.E. & Sparke, L.S. 1998, ApJL, in press (astro-ph/9803146).

Loose, H.-H. & Thuan, T.X. 1985 in *Star-forming Dwarf Galaxies* (D. Kunth, T.X. Thuan & J. Tran Than Van, eds.), Gif sur Yvette: Editions Frontieres, p. 73.

Marlowe, A.T., Meurer, G.R. & Heckman, T.M. 1997, ApJS, 112, 285.

Martin, C. 1997, ApJ, 491, 561.

Martimbeau, N., Carignan, C. & Ray, J.-R. 1994, AJ, 107, 543.

Matthews, L.D. & Gallagher, J.S. 1997, AJ, 114, 1899.

McGaugh, S.S., Schombert, J.M. & Bothun, G.D. 1995, AJ, 109, 2019.

Miller, B.W. & Hodge, P. 1994, ApJ, 427, 656.

Patterson, R.J. & Thuan, T.X. 1996, ApJS, 107, 103.

Phillipps, S. & Disney, M. 1985, MNRAS, 217, 435.

Puche, D., Westphal, D., Brinks, E. & Roy, J.-R. 1992, AJ, 103, 1841.

Schmidt, M. 1959, ApJ, 129, 243.

Strobel, N.V., Hodge, P. & Kennicutt, R.C. 1991, ApJ, 383, 148.

Tresse, L. & Maddox, S.J. 1998, ApJ, 495, 691.

van Zee, L. 1996, PhD thesis, Cornell University.

### Figure captions

- Figure 1: Examples of galaxies of different types and morphologies. Each row shows the galaxy as imaged through the H $\alpha$  filter at left, through the continuum filter at the center, and in the net-H $\alpha$  line at right. The galaxies are VCC 17 (E & A), VCC 1374 (L, Sp & S), and VCC 10 (C & S). A 10 arcsec bar at the upper right corner of each row sets the scale.
- Figure 2: Distribution of classification indices for DIGs. Each independent classification is represented by a circle. The points in regions of high concentration have been “jiggled” slightly in an attempt to separate points which are very close together. Concentration index values of 100 represent galaxies with CI= $\infty$  (*i.e.*, all HII regions in central locations).
- Figure 3: Distribution of classification indices for DIGs. This is an expansion of Figure 2 near CI $\simeq 0$ . The points have **not** been jiggled in this presentation.
- Figure 4: Distribution of the asymmetry index among galaxies which have CI $\neq \infty$ . Most of the objects concentrate in the low AI bins, indicating a preference for asymmetric distribution of HII regions.

Table 1. Location of HII in irregular galaxies

Galaxy	Type	CI	S/A.	AI	Ref.	Galaxy	Type	CI	S/A.	AI	Ref.
U300	E	0	A	0.5	1	U191	E	0	A	0.58	2
U521	C	100	S	1	1	U634	E	0	A	0	2
U2684	E+C	100	A	1	1	U891	L, Sp	100	S	1	2
U2984	E, El	0	A	0.38	1	U1175	E	0	A	0	2
U3174	E	1.33	A	0.4	1	U2162	E	0	A	0.5	2
U3672	E	0	A	0	1	U3050	C+E	1.33	A	0.5	2
U4660	D	0	A	0.33	1	U4762	E	0	A	0.5	2
U5716	E, El	0	A	0	1	U5764	C+E	0	A	0	2
U7178	C+E	0.67	A	0.17	1	U5829	E	0	A	0	2
UGCA357	E	0	A	0	1	U7300	E	0	A	0.33	2
HARO43	L, Sp	2	S	1	1	U8024	E	0	S?	0.29	2
U9762	D?	-	?	-	1	U9128	E	0	S	0	2
U10281	E	0	A	0	1	DDO210	C	100	S	0	2
U11820	E	0.87	A	0.58	1	N1427A	E	0.2	A	0.11	4
97073	E, El	0.31	A	0	3	V0017	E	2	A	0.5	7
97079	E	0	A	0	3	V0169	E	0	A	0.5	7
97087	L, Sp	1	A	1	3	V0217	E	0	A	0.5	7
97138	E	0.66	A	0.25	3	V0328	E	0	A	0.5	7
108085	E	0	A	0	3	V0350	C?	0	S	0	7
127037	E, El	0.57	A	0.20	3	V0477	E	0	A	0	7
160086	C	0.57	S	0.75	3	V0530	C	100	A	0	7
160139	E	0	A	0.22	3	V0826	E	0	A	0.5	7
HARO 14	C	100	A	1	5	V0963	C	100	S	0	7
N625	C	100	S	1	5	V1455	C	100	A	0	7
N1510	C	100	S	1	5	V1465	C+E	2.5	A	0	7

Table 1—Continued

Galaxy	Type	CI	S/A.	AI	Ref.	Galaxy	Type	CI	S/A.	AI	Ref.
N1705	C	100	S	1	5	V1468	E	0	A	1	7
N1800	C+E	1	S	0	5	V1585	E	0	A	0	7
N2101	C+E	0.33	S	0.23	5	V1753	E	0	A	0	7
II Zw40	C	1	S	1	5	V1952	E	0	A	0	7
N2915	C+E	100	A	0.66	5	V1992	E	0	A	0	7
N3125	C+E	1	A	1	5	V2034	D?	-	?	-	7
N3955	C	100	A?	1	5	V0010	C	100	S	1	8
N4670	C	100	S	1	5	V0144	C	100	S	1	8
N5253	C	100	S	1	5	V0172	C+E	0	A	0	8
N1569	C	1	S	0.33	6	V0324	C	100	S	1	8
N1800	E	100	A	1	6	V0410	C	100	S	1	8
II ZW 40	C	1	S	0.25	6	V0459	E	0	A	1	8
N2363	C	100	S	1	6	V0513	C	100	S	1	8
I ZW 18	C	4	S	0	6	V0562	C	100	S	1	8
M82	C	100	S	1	6	V0985	E	100	A	1	8
N3077	C	100	S	1	6	V1179	C	100	S	1	8
SEX A	E	?	A	?	6	V1374	L, Sp	2	A	1	8
N3738	C	100	A	1	6	V1725	L, Sp	4	A	0	8
N4214	L, Sp	0.5	S?	0.33	6	V1791	E	0	A	0.5	8
N4449	L, Sp	?	A	?	6	Ho II	C	1	S	1	9
N5253	C	100	S	1	6	DDO 47	D	1.28	S	0.89	10
Ho I	E	0.13	A	0.35	11	Sex B	E	0.36	A	0.5	10
Ho IX	E	0	A	0.20	11	DDO 167	C	25	A	0.66	10
IC 2547	E	0	A	~0.5	11	DDO 168	L, Sp	1	S	0.71	10
M81dB	L, Sp	0.25	S	0.33	11	DDO 187	E	0	A	0.5	10



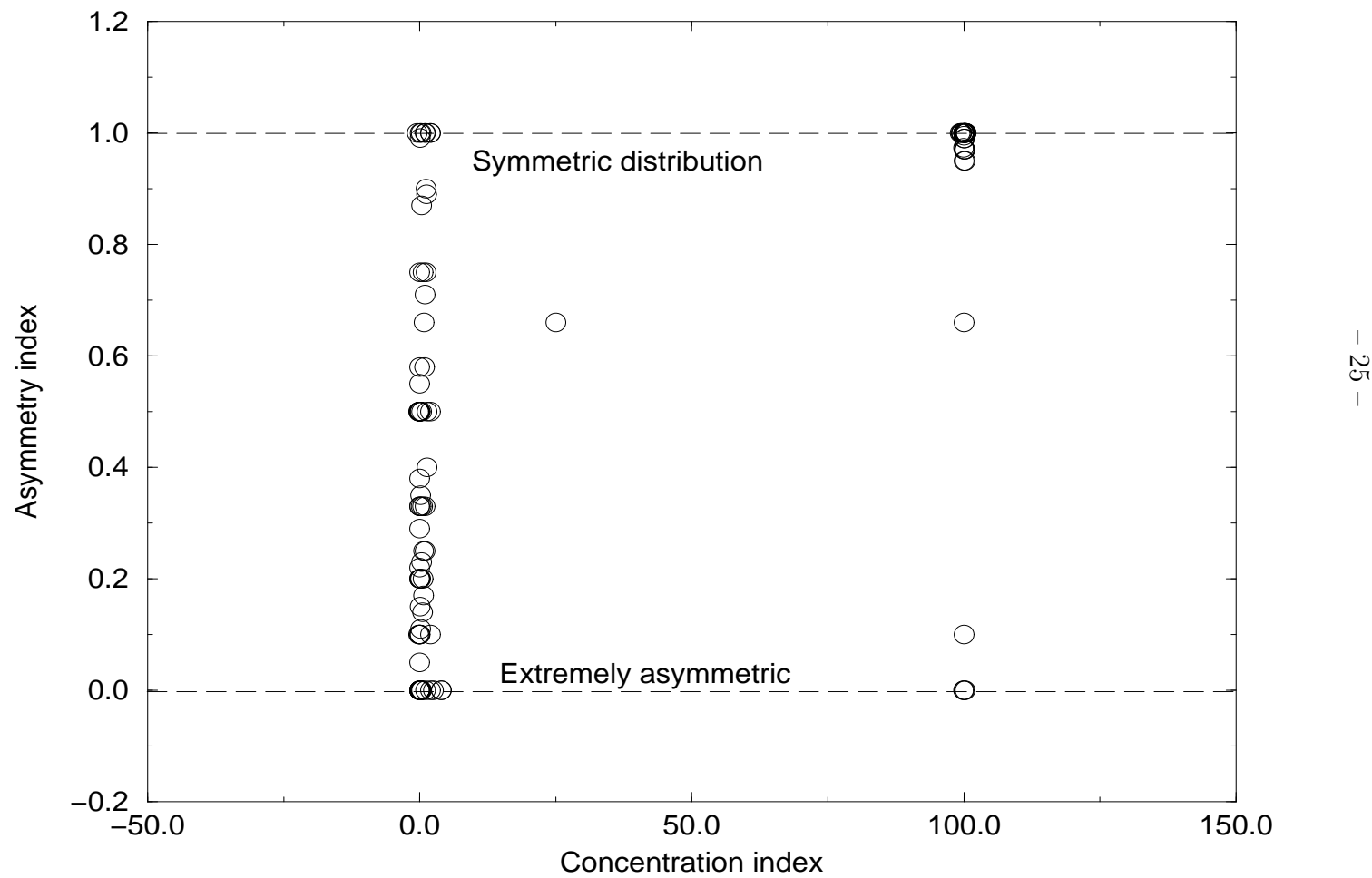
Table 1—Continued

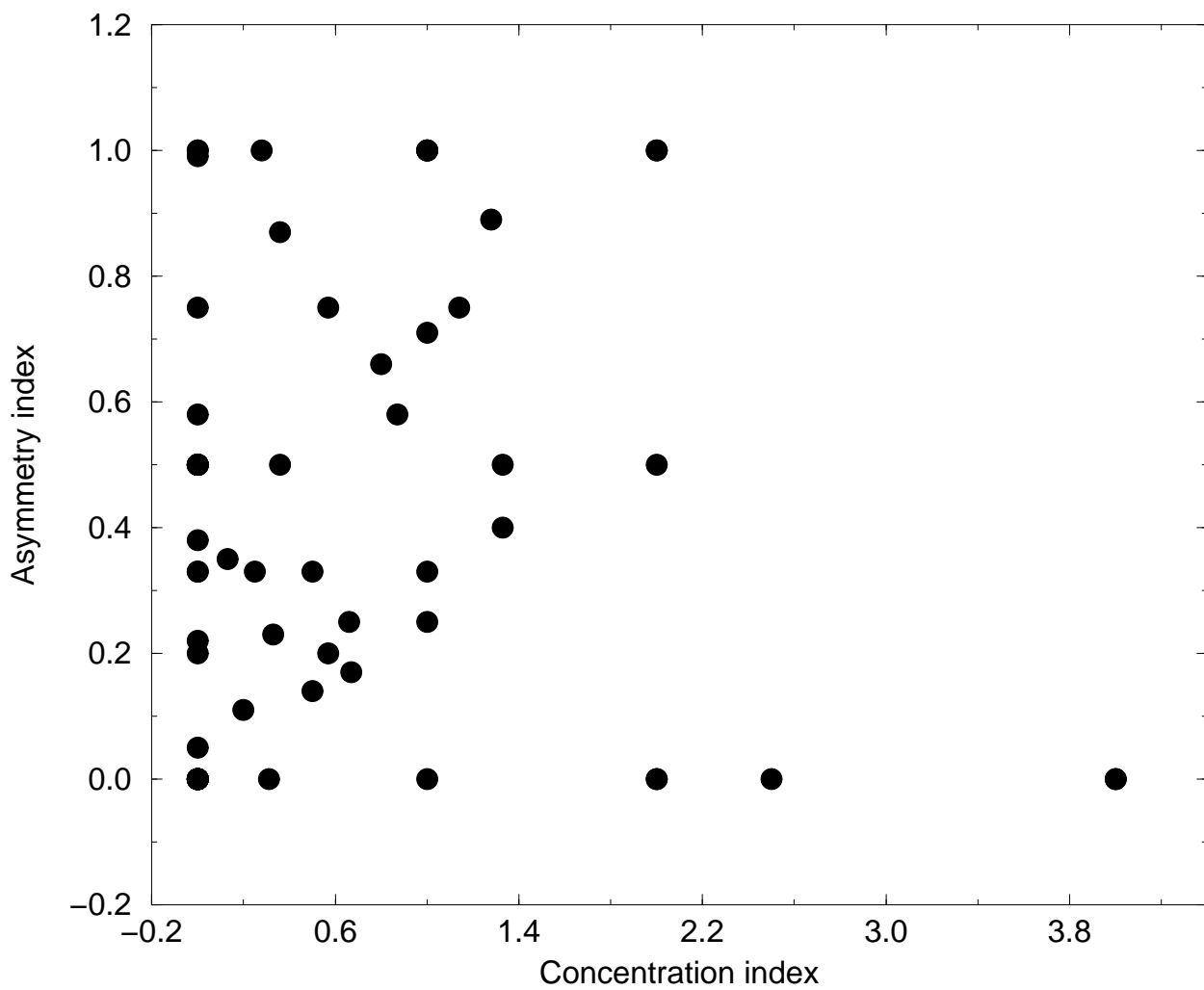
Galaxy	Type	CI	S/A.	AI	Ref.	Galaxy	Type	CI	S/A.	AI	Ref.
F415-3	C	2	A	0	12	F469-2	C+E	2	A	0	12
F561-1	E	1.14	A	0.75	12	F563-V1	D	100	S	1	12
F611-1	E	0	A	0	12	U12695	E	0.5	A	0.14	12
F562-V2	C+E	0	A	0.5	12	F746-1	E	0.36	A	0.87	12
U5709	C	100	S	1	12	F568-1	C+E	0.28	S	1	12
F583-5	L, Sp	0	S	0.75	12	F585-3	C	0.8	S	0.66	12
U5675	C	0	S	1	12						

Note. — The second column gives the typology for the location of the HII regions with the following coding: E=egde, C=center, S=scattered, D=diffuse, El=on (part of) ellipse, L=Linear, Sp=spine. The numerical concentration index CI, defined in the text, is given in column 3. The symmetry classification is given in column 4, while the asymmetry classifier AI is given in column 5.

Table 2. References for classification images

No.	Reference	Galaxies
1	van Zee 1996 primary	14
2	van Zee 1996 secondary	13
3	Gavazzi <i>et al.</i> 1998	8
4	Hilker <i>et al.</i> 1998	1
5	Marlowe <i>et al.</i> 1997	12
6	Martin 1997	12
7	Heller <i>et al.</i> 1998	17
8	Almoznino & Brosch 1998	13
9	Puche <i>et al.</i> 1992	1
10	Strobel <i>et al.</i> 1991	4
11	Miller & Hodge 1994	4
12	McGaugh <i>et al.</i> 1995	13
Total number of images		113





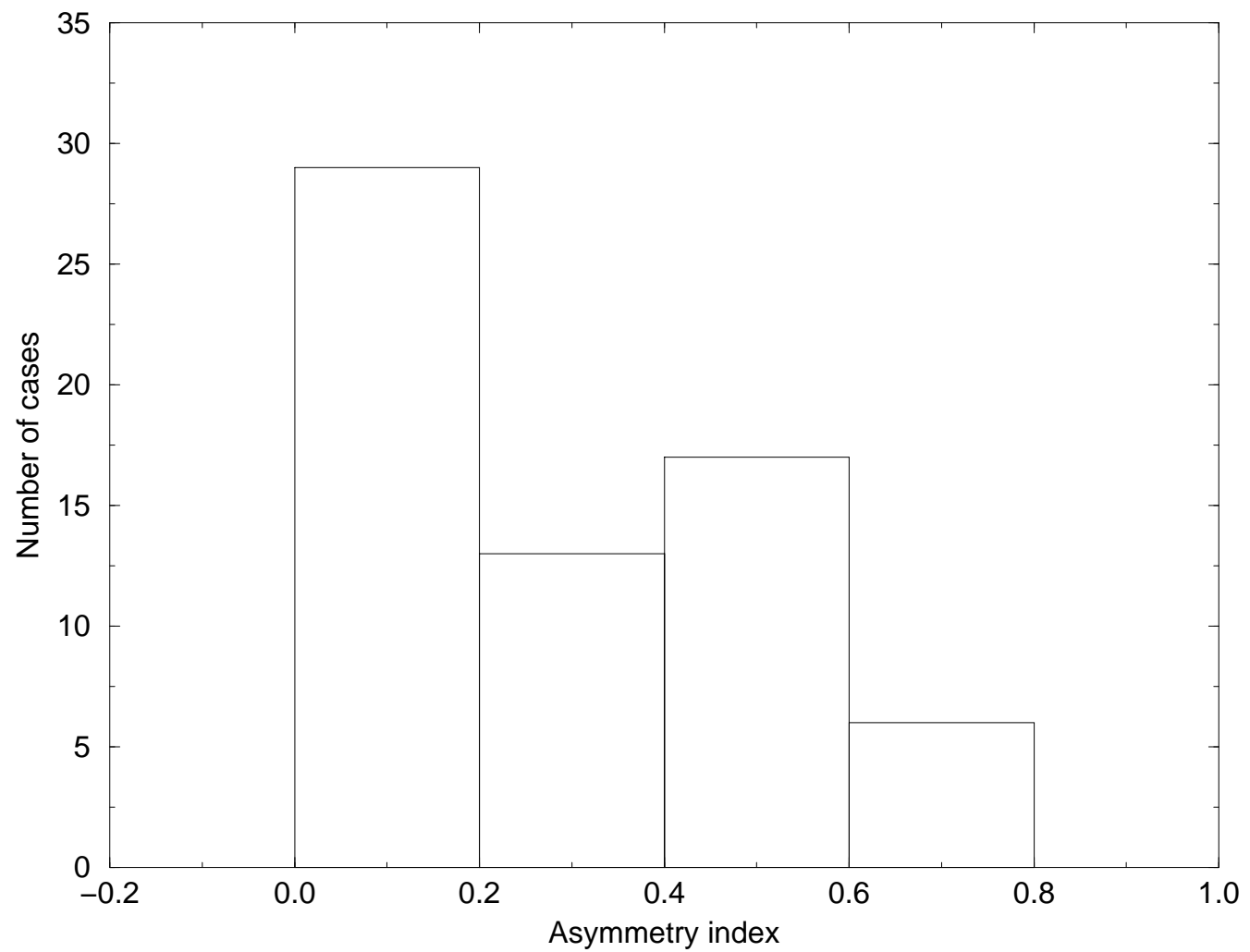


Table 3. Statistics of types and morphology

Distribution	S morphology	A morphology	Total
E	5	57	62
D	2	1	3
L	6	4	10
C	32	17	49
Total	45	79	124

Note. — Galaxies with mixed morphology are counted once in each bin (double counting).

